Skarn formation and Cu—Ag mineralization in the McKenzie Gulch area, northern New Brunswick, Canada: Implication for the applications of mineral chemistry in exploration for porphyry copper and skarn deposits

Ronald J. Massawe [a,b,c,*], David R. Lentz [b]

[a] Geological Survey of Tanzania, P.O. Box 903, Dodoma, Tanzania
[b] Department of Earth Sciences, University of New Brunswick, 2 Bailey Drive, Fredericton, NB E3B 5A3, Canada
[c] Department of Geosciences, School of Mines and Geosciences, University of Dar es Salaam, P.O. Box 35052, Dar es Salaam, Tanzania

ABSTRACT

The McKenzie Gulch (MG) copper–silver skarn occurrences are associated with the Middle Devonian intermediate to felsic dyke swarms. Mineralization occurs as veins and stockwork of veinlets, disseminations, patchy, and locally as replacement of calc-silicate skarns in argillaceous limestone. This skarn is interpreted to have developed in three stages: the earliest contact metamorphic stage resulting in hornfels developed from calcareous mudstone and very fine-grained clastic sedimentary rocks (Stage I); this was followed by metasomatic replacement resulting in prograde anhydrous skarn containing grossular-andradite (grandite), diopsidic pyroxene, and wollastonite (Stage II); increasing fluid/rock interaction results in retrograde skarn dominated by epidote, calcite, green amphibole, chlorite, sulfide minerals, titanite, andradite and hedenbergite commonly along veins and veinlets (Stage III). Subordinate sphalerite and pyrite occur in late veins cross-cutting both porphyry dykes, skarns and hornfels zone.

Prograde garnets in the study area belong to the grossular-andradite solid solution that ranges from $Adr_{16}Gr_{82}$ to almost pure andradite - $Adr_{99}Gr_1$, whereas other garnet end-members constitute less than 5% collectively. Pyroxenes form a diopside-hedenbergite solid solution with composition between $Di_{31}Hd_{60}$ and $Di_{93}Hd_7$, while other pyroxenes constitute less than 10% collectively. These garnets and pyroxenes exhibit chemical zonation patterns generally characterized by a rim of Fe enrichment relative to cores of grains, which may suggest possible change in salinity (or other factor that promotes Fe transport). This means grossular and diopsidic cores are rimmed by more andradite and hedenbergitic compositions for garnet and pyroxene, respectively. In general, there is a tendency for increasing Fe component in both garnet and pyroxene from the prograde to retrograde stages.

Epidote formed during the retrograde stage exhibits oscillatory zoning similar to retrograde andradite and indicates Fe enrichment increasing from core to rim. Based on the major element composition, textural and optical characteristics of garnets, we conclude that grandites (Al-rich) formed under low water/rock ratios, in equilibrium with metasomatic fluids whose composition was locally buffered by the host rocks, whereas andradite (Fe-rich) resulted from relatively high water/rock ratios that were in equilibrium with a magmatic-derived fluid. The results of this study indicate that there is a relationship between the composition of pyroxenes and garnets of the skarn alteration facies and the dominant metal of the mineralized skarns. These facies plot in the compositional field of Cu-dominated skarns. As a result, this relationship may be applied in exploration for skarn and porphyry copper mineralization.

1. Introduction

The McKenzie Gulch (MG) Cu—Ag skarns occur in the northern New Brunswick and belong to the northern Appalachian porphyry-skarn systems that include the Gaspé Peninsula, Québec and the northern Maine, USA (Fig. 1; Hollister et al., 1974; Hollister, 1978; Allcock, 1982;

Williams-Jones, 1982; Wares and Brisebois, 1998). Other occurrences in the region include the Mines Gaspé and Mines Madeleine deposits in Québec and several polymetallic Cu-Pb-Zn-Ag-Au prospects that have been the subject of detailed mapping and sampling in the past four decades (Girard, 1971; Shelton and Rye, 1982; Shelton, 1983; Savard, 1985; Procyshyn, 1987; Malo et al., 1993; Malo et al., 2000).

In northern New Brunswick abundant contact metasomatic Cu—Au skarn deposits are proximal to small Siluro–Devonian intermediate to felsic intrusions (Lentz et al., 1995). Copper–silver skarn mineralization in the MG area have been identified in four zones: the Woden Brook occurrence to the northeast, the McKenzie Gulch and the Legacy skarn occurrences in the central part of the area, and the Burntland Brook occurrence to the southwest (Fig. 2). These skarns occur between two major dextral-slip fault systems, the McKenzie Gulch Fault and the Rocky Gulch Fault to the west and east, respectively (Fig. 2). All four occurrences are hosted by Matapédia Group calcareous sedimentary rocks of the Upper Ordovician to Lower Silurian. These skarns are spatially associated with swarm of sub-vertical northeast-trending Devonian intermediate to felsic dykes (Moore and Lentz, 1996).

Most skarn deposits exhibit an intimate spatial relationship with intrusions; consequently, skarn minerals can recorded the fluid(s) that were present in the intrusive environment during ore skarn formation (Meinert et al., 2003). Two distinct mineral assemblages are common in skarns: 1) an early prograde stage containing anhydrous minerals (e.g., garnet and pyroxene), which forms from relatively high-temperature, hypersaline liquid (cf. Kwak, 1986), and 2) late retrograde stage containing hydrous minerals (e.g., epidote, amphibole, and chlorite), and forms from lower temperature, lower salinity fluids (Kwak, 1986). The later stage hydrous assemblage is commonly associated with ore minerals (Cu—Ag sulfides) and is considered to be the main mineralizing

stage in most skarn systems.

The relationship between the composition of pyroxene and garnet within the skarn and the dominant metals has been discussed by several authors (e.g., Meinert, 1983; Ray and Webster, 1997; Malo et al., 2000). This study presents information from geological mapping, drill core logging, petrographic examination and mineral chemical analysis of prograde and retrograde assemblages to constrain skarn development and hydrothermal alteration during magmatic-hydrothermal processes that resulted in the formation of Cu—Ag skarn and Au-vein type mineralization. Garnets from this study have a composition that falls along the grossular–andradite solid solution, and plot in the compositional field of Cu-dominated skarns. Likewise, pyroxene composition falls between diopside and hedenbergite solid solution, and plot in the field of typical Cu-dominated skarns like garnets.

2. Geologic setting

2.1. Regional geology

The MG area is part of the Aroostook-Matapédia Cover Sequence (AMCS) (Fyffe and Fricker, 1987) also known as the Gaspé Belt (Bourque et al., 1995) that represent an old and broad depositional belt in the northern Appalachian. This is underlain by clastic and subordinate calcareous sedimentary rocks that range from Upper Ordovician to Lower Silurian (Figs. 1 and 2). The AMCS covers an area between Gaspé Peninsula, northern New Brunswick and Maine, USA and overlies the Taconian-deformed Cambrian to Ordovician rocks that belong to Dunnage Zone. The same belt (AMCS) has been divided into Connecticut Valley – Gaspé Synclinorium (CVGS), Aroostook – Percé Anticlinorium (APA), and Chaleurs Bay Synclinorium (CBS) based on their
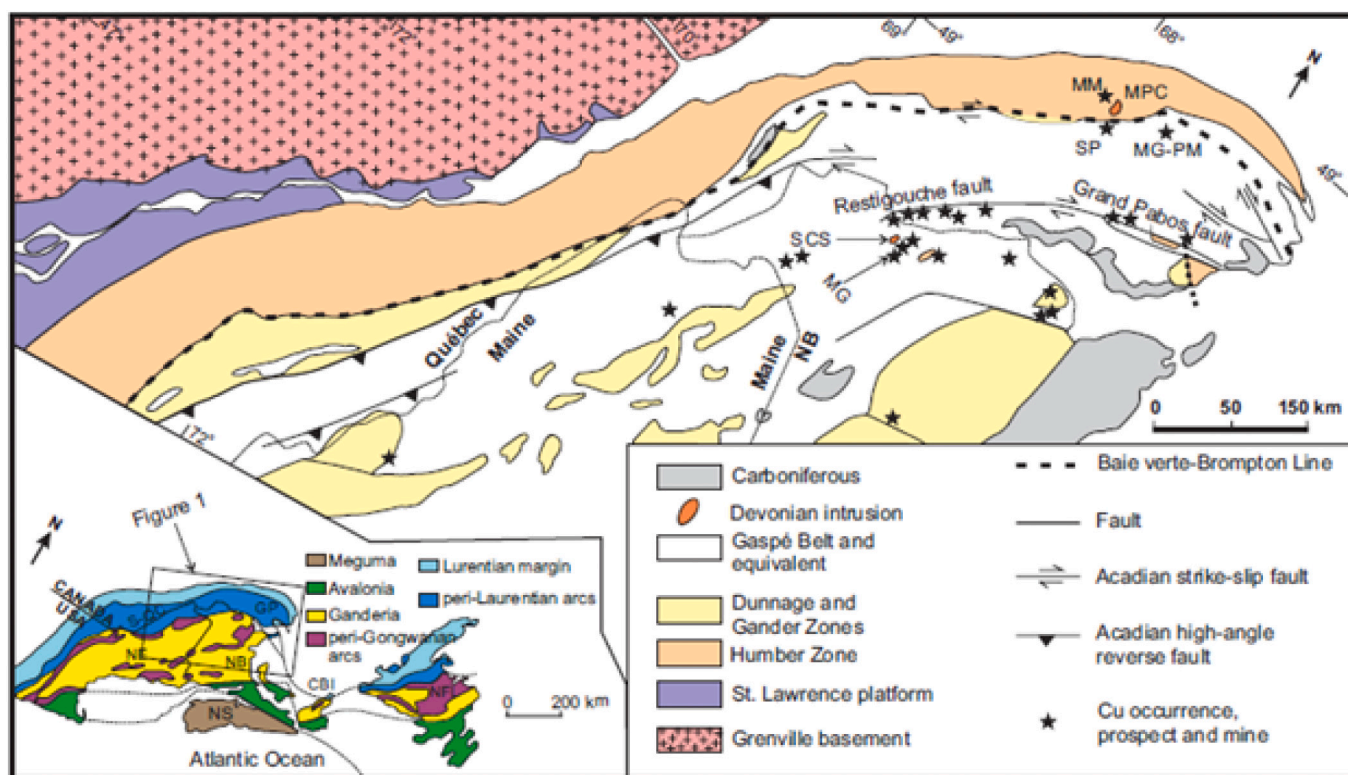
Fig. 1. Simplified geologic map of the Québec-New England-New Brunswick sector of the northern Appalachians modified from Malo et al. (2000). Porphyry Cu and Cu skarn deposits are compiled from Hollister et al. (1974), Williams-Jones (1982), Savard (1985), Roy (1991), Malo et al. (1993), Lentz et al. (1995), Moore and Lentz (1996). Abbreviations: GP = Gaspé Peninsula, MG-PM = Mines Gaspé–Copper and Porphyry Mountains, MM = Mines Madeleine, MPC = McGerrigle plutonic complex, SCS = Squaw Cap stock, SP = Sullipek prospect, NB = New Brunswick, NE = New England, NF = Newfoundland, NS = Nova Scotia, CBI, Cape Breton Island; NFL, Newfoundland S-QC = southern Québec. The northern Appalachian inset map is comprised of tectonostratigraphic divisions in the Canadian Appalachians modified after Hibbard et al. (2006).

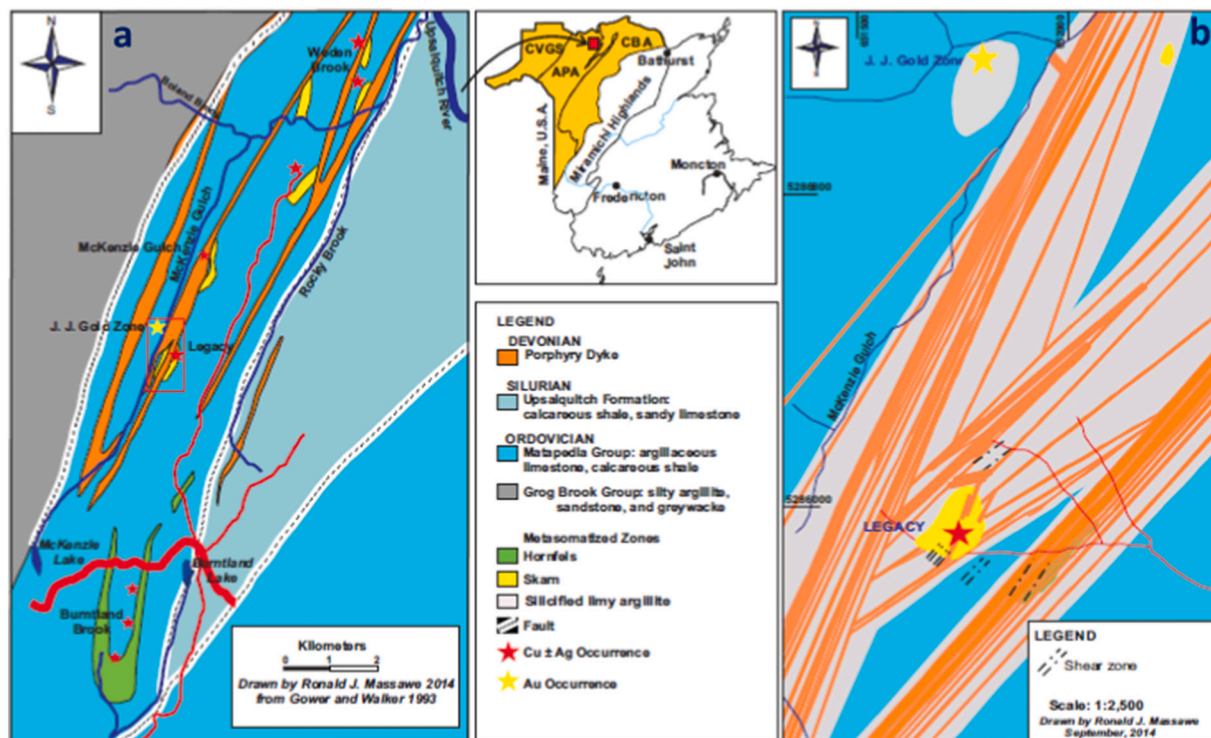**Fig. 2.** Geology of the McKenzie Gulch area: a) the location of the Legacy McKenzie Gulch deposit with respect to other Cu—Ag skarn in the area. Modified from Gower and Walker (1993); Wilson and Kamo (2008). Area of (a) is located on the inset map, and b) detailed geology of the Legacy McKenzie Gulch deposit (MG) this study.

tectonostratigraphic affinities (Bourque et al., 1995; Fig. 2). Chronologically, the APA appear to have the oldest rocks that include a Grog Brook Group (lower siliciclastic) and a Matapédia Group (overlying calcareous unit), which together form a turbidite sequences that represent a gradual infilling of the fore-arc basin (Salinic). The CBS occur to the east of APA and comprises of Silurian and Devonian rocks that include Aeronian to lower Lochkovian rocks of the Chaleurs Group, Lower Devonian rocks of the Dalhousie and Tobique groups and Campbellton Formation (Wilson and Kamo, 2008; Wilson, 2017).

Wilson (2017) and others have divided the Matapédia Group rocks into the White Head Formation and the Pabos Formation. The latter in New Brunswick is considered to be a transitional lithological unit between underlying siliciclastic rocks of the Whites Brook Formation (Grog Brook Group), and overlying calcareous rocks of the White Head Formation (Matapédia Group; Fig. 2). It consists of two dominant lithological facies in northern New Brunswick: 1) a sandstone turbidite association consisting of light grey, weakly to strongly calcareous, thin- to medium-bedded, medium- to coarse-grained sandstone and siltstone, intercalated with dark grey calcareous shale and minor conglomerate; and 2) a calcareous siltstone association comprising thin-bedded (0.2–4.0 cm), medium- to dark-grey or greenish grey, calcareous, parallel-laminated siltstone or mudstone, interstratified with thin beds (2–6 cm) of calcareous to non-calcareous, fine-grained sandstone, and medium- to dark-grey calcilutite or shaly calcilutite (Wilson, 2002; Carroll, 2003; Wilson et al., 2004; Wilson, 2017).

The White Head Formation is a carbonate mudstone flysch sequence constituting the upper part of the Matapédia Group. The White Head Formation consists of thinly interbedded (0.5–5.0 cm) medium- to dark-grey, very fine-grained calcilutite (carbonate mudstone) and calcareous shale or siltstone. Together these rocks form a distinct macroscopic texture that has been referred to as 'ribbon rock' or 'ribbon limestone' (Woods, 1993; Wilson, 2017). The 'ribbon' appearance have been enhanced by differential weathering of more resistant shaly beds relative to less resistant calcitic or ankeritic calcilutite beds. Thin (0.5–10.0

cm) interbeds, lenses, or laminae of fine-grained calcarenite, calcareous sandstone, or calcareous siltstone are also normally present (Wilson, 2017). Much of the White Head consists of thin-bedded, fine-grained calcilutite with planar contacts and microlaminations, commonly alternating with thin beds of mudstone or shale, similar to 'muddy contourites' and hemipelagic slope sediments (Stow and Lovell, 1979; McIlreath and James, 1984).

2.2. Geology of the McKenzie Gulch area

The Grog Brook Group represents the oldest rocks in the study area. The common rocks in this group include greywacke, sandstone, and silty argillite. The MG skarn occurrences are hosted by Matapédia Group rocks that are separated from Grog Brook Group rocks to the northwest by the McKenzie Gulch Fault. The younger Chaleurs Group rocks occur to the southeast of the Matapédia Group and separated by Rocky Gulch Fault. Middle Devonian felsic dykes with slab failure signature (Massawe and Lentz, 2019) occur throughout the MG area, where they intrude the Matapédia Group rocks, and are commonly concentrated in swarms (Fig. 2). These dyke swarms range from intermediate to felsic in composition (Moore and Lentz, 1996; Massawe and Lentz, 2019), and represent both weakly and highly altered components of the intrusive suites in the study area. Igneous textures in the highly altered dykes are almost completely obliterated and igneous mineralogy has been replaced by secondary mineral assemblages, such as sericite, clay, calcite, and chlorite (Massawe and Lentz, 2019). This alteration also represents bleaching that introduces a white coloration in some dykes and results from abundant clay minerals and subordinate secondary quartz.

Contact metamorphic aureoles consisting of fine- to medium–grain greenish grey hornfels, white to grey marble, dark to light green calcic hornfels are common adjacent and parallel to dyke swarms in the study area (Fig. 3). Compositionally, these metamorphic aureoles consist of patchy garnet and pyroxene skarn within parallel or discordant veins or
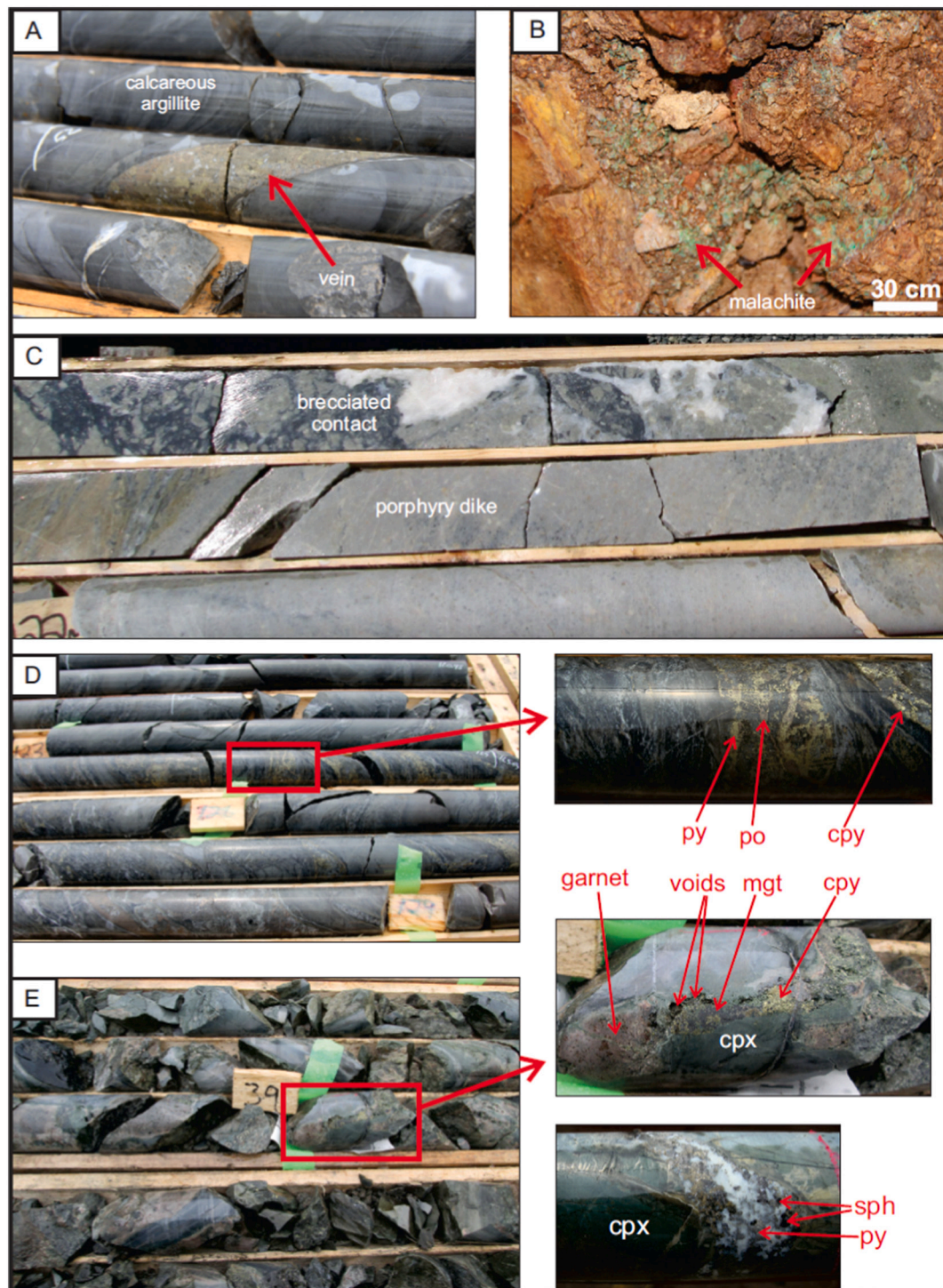
Fig. 3. Core photographs of samples from the MG skarn and adjacent Au-bearing quartz veins: (A) calcareous argillite cross-cut by Au-bearing quartz-calcite-sulfide vein; (B) typical surface oxidation of Au-bearing veins from (A); (C) porphyry dike with brecciated texture near skarn-calcareous argillite contact; (D) skarn with stockwork mineralization; (E) sheared/broken hornfels with an alternating bands of green fine-grained clinopyroxene (cpx) and pinkish-brown garnet. The latter bands contain magnetite (Mgt), chalcopyrite (Cpy) and minor pyrite = Py and pyrrhotite = Po. Voids may have resulted from replacement of garnet by sulfides and magnetite. Late veins rich in sulfides (sphalerite = Sph, pyrite = Py, ± chalcopyrire) cross-cut these hornfels as well; (F) magnetite-bearing hornfels cross-cut by a porphyry dike with contacts labelled C; (G) banded skarn with late and barren quartz-calcite veins representing retrograde stage; (H) skarn with spotted texture of the retrograde assemblage; (I) porphyry dike in contact with skarn and mineralization concentrated at the contact. Late and mineralized veins cross-cutting porphyry dike; (J) slab photograph representing an endoskarn zone and marble; (K) slab photograph representing prograde facies (garnet = grt, clinopyroxene – not in photo) replaced by retrograde facies (amphibole = amph, chlorite = chl, calcite = cc); see text for details. Cores (NQ) diameters in all is 4.8 cm. (For interpretation of the references to colour in this figure legend, the reader is referred to the web version of this article.)
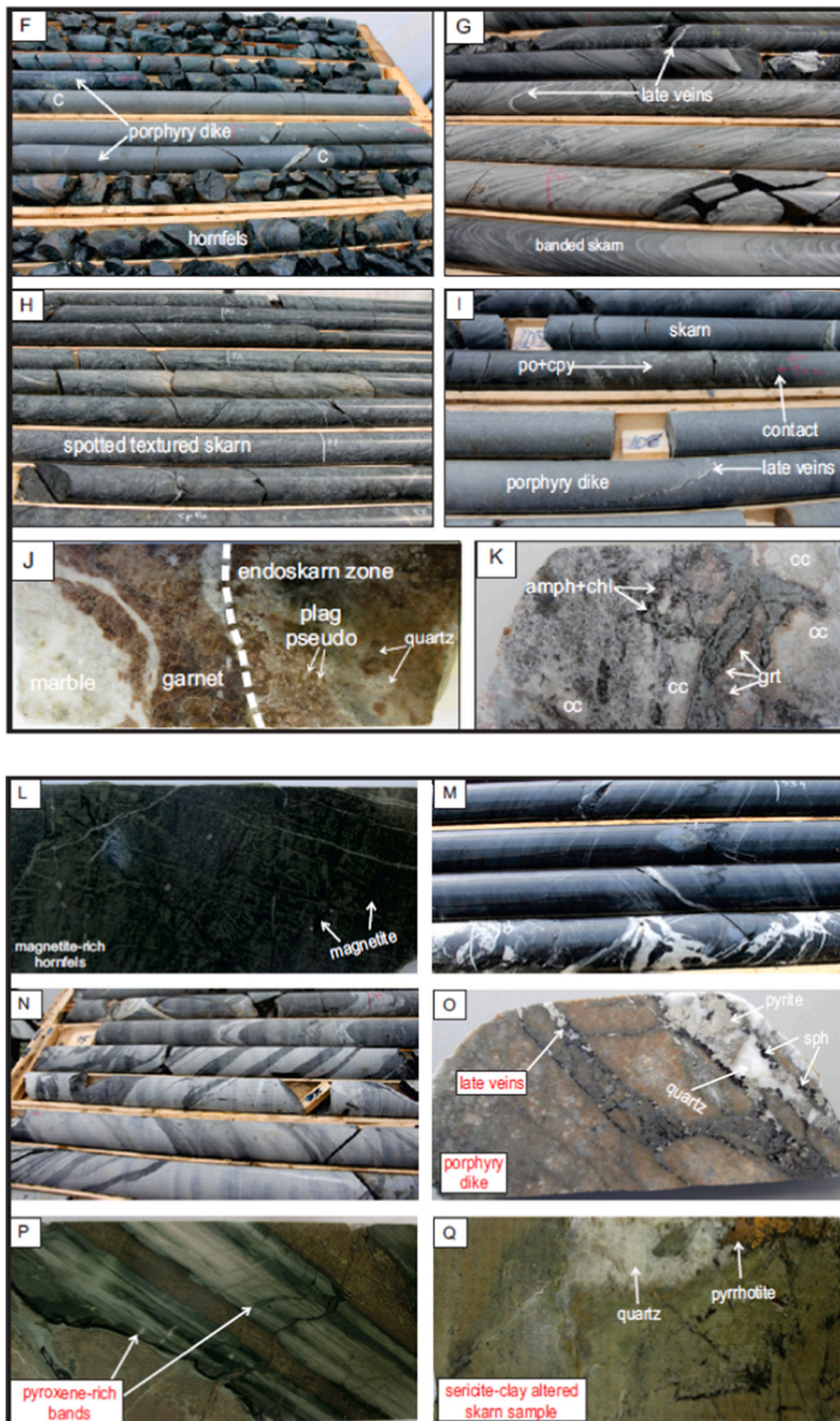
Fig. 3. (continued).

as thick patchy layers (Woods, 1993). Copper–silver mineralization in the study area is commonly associated with retrograde assemblage of epidote, amphibole, chlorite, calcite, quartz, and minor vesuvianite (Fig. 4), but subordinate amount may occur within coarse-grained garnet and pyroxene skarn as replacements of the same minerals. This mineralization occurs in three zones: the Legacy deposit (1,500,000 t of
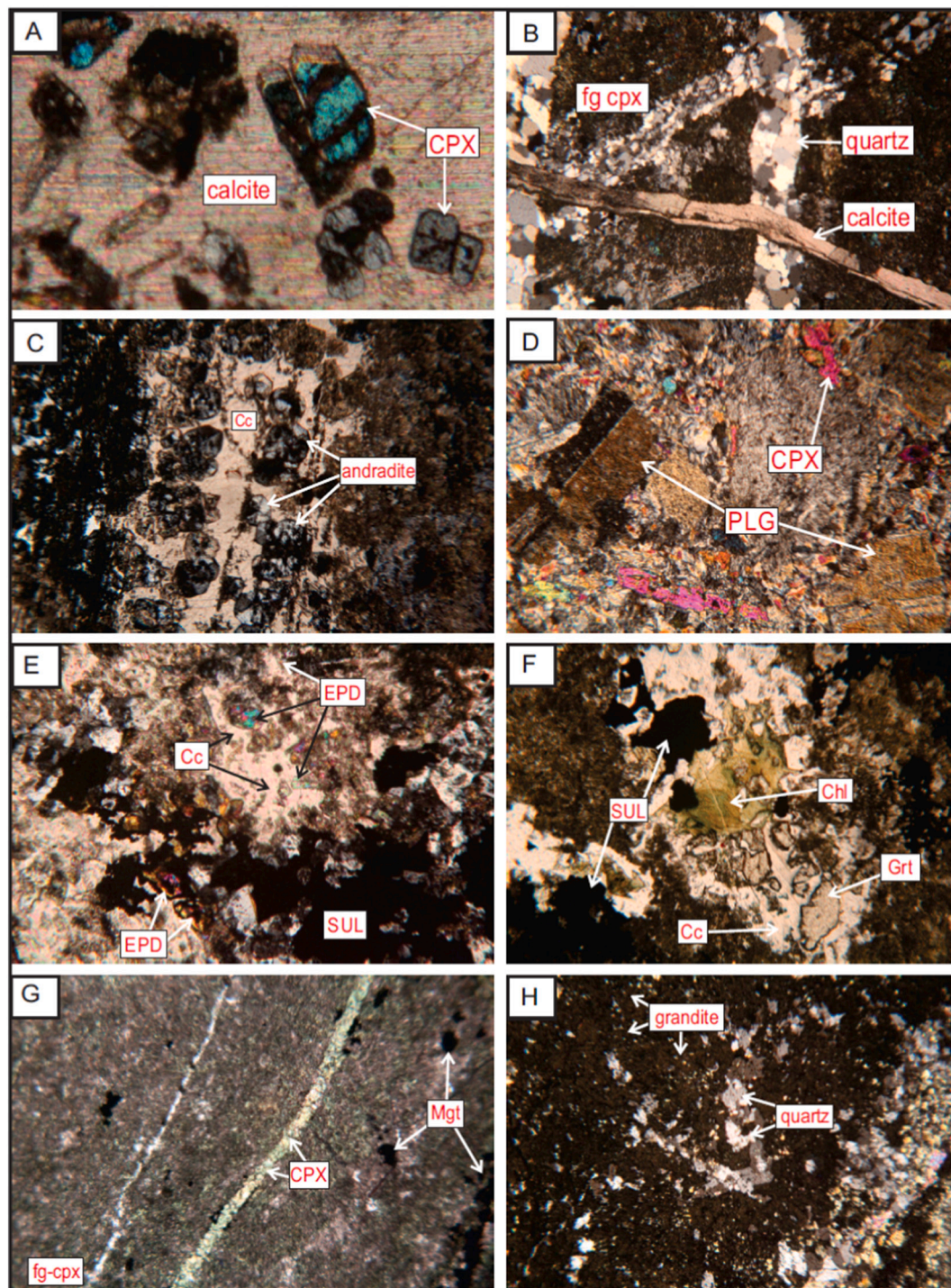
Fig. 4. Photomicrographs (A-K) and Backscatter Scanning Electronic Microprobe (BSE-SEM) images (L-P) of representative samples from the MG skarns: (A) late clinopyroxene (CPX) included in large hydrothermal calcite crystal (XPL); (B) fine-grained clinopyroxene hornfels cross-cut by late stage calcite and quartz veins; (C) prograde skarn cross-cut by late andradite- and calcite-bearing vein (XPL); (D) endoskarn zone with plagioclase (PLG) pseudomorphs and clinopyroxene (CPX; XPL); (E) retrograde skarn with epidote (EPD) and calcite (Cc) both associated with sulfides (SUL) (XPL); (F) retrograde skarn with chlorite (Chl) replacing garnet (Grt; XPL); (G) fine-grained magnetite (Mgt)-bearing clinopyroxene (fg-cpx) hornfels with cross-cutting late clinopyroxene (CPX) vein (PPL); (H) prograde grossular-andradite (grandite)-bearing skarn along with quartz and fine-grained clinopyroxene (PPL); (I) retrograde skarn with chlorite replacing garnet both associated with hydrothermal titanite (PPL); (J) retrograde alteration assemblage quartz-sericite-calcite and late clinopyroxene-titanite (XPL); and (K) clinopyroxene hornfels cross-cut by late skarn veins with late garnet-calcite-clinopyroxene (XPL); (L) zoned andradite with microfractures which represent early retrograde skarn; (M) zoned epidote crystals of retrograde stage; (N) prograde skarn with diopside (Di), grossular-andradite (grandite), and wollastonite (Wo); (O) retrograde amphibole; and (P) hedenbergite representing early retrograde skarn. Abbreviations: XPL = cross polarized and PPL = plane polarized. Field of view, where no scale bar is 5 mm.
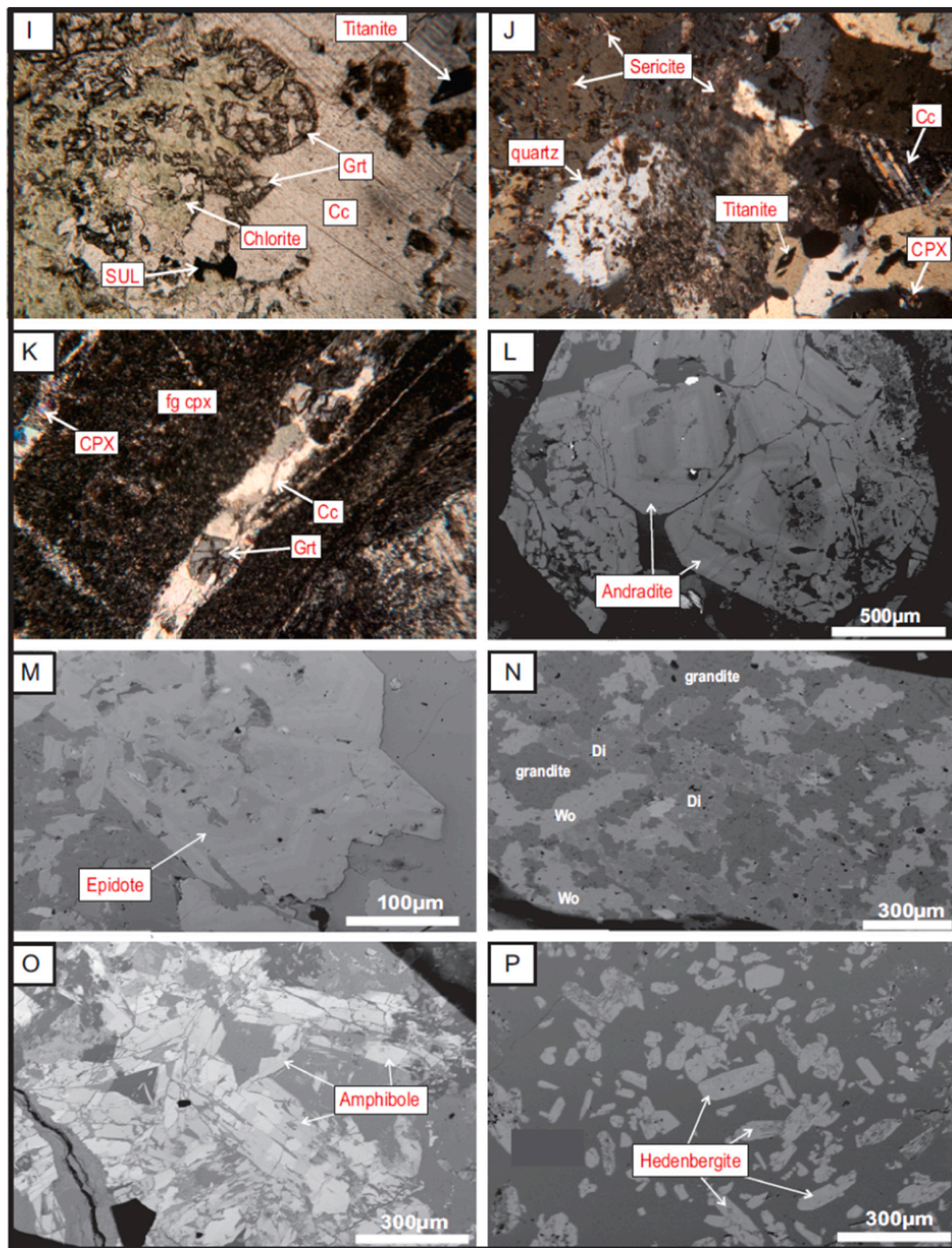
Fig. 4. (*continued*).

0.87% Cu and 10.29 g/t Ag) at the center), the Woden Rock Brook (0.5% Cu over 6.0 m) and McKenzie Gulch (1.11% Cu and 10.63 g/t Ag over 0.5 m) occurrences to the northeast, and the Burntland Brook occurrence (0.40% Cu over 10.2 m) to the southwest.

3. Materials and methods

Electron microprobe analysis of prograde (garnet, pyroxene, and wollastonite) and retrograde (epidote, amphibole, and vesuvianite) skarn assemblages from MG was carried out at the University of New Brunswick Microscopy and Microanalysis Facility, using the JEOL JXA-733 EPMA equipped with dSspec and dQant32 automation (Geller Microanalytical Laboratories). The instrument was operated with an accelerating voltage of 15 kV, and a probe current of 30 nA. Counting times on peaks were 30 s, except for sulfur (60 s) and high and low backgrounds were each counted for 15 s. Backscattered electron images were obtained with dPict32 (Geller Microanalytical Laboratories). A variety of synthetic and natural standards were used for monitoring analytical accuracy. These include: orthoclase, jadeite, bytownite, bustamite, olivine, ilmenite, hematite, Cr metal, CPX511 for clinopyroxene, amphibole, and vesuvianite with an additional three standards (barite, tremolite and tugtupite) for the latter two minerals. Clinopyroxene and amphibole crystals were analyzed for ten and thirteen elements, respectively at the following detection limits: Na (136 ppm), Mg (89 ppm), Al (73 ppm), Si (87 ppm), K (93 ppm), Ca (102 ppm), Fe (416 ppm), Mn (245 ppm), Ti (108 ppm), Cr (140 ppm), Ba (1282 ppm), F

(199 ppm), and Cl (104 ppm).

The concentration of the following eight elements, with their respective detection limits in brackets, were analyzed in garnet: Si (78 ppm), Mg (81 ppm), Al (76 ppm), Ca (73 ppm), Fe (380 ppm), Mn (316 ppm), Cr (161 ppm), and Ti (127 ppm), whereas epidote were analyzed for twelve elements Mg (75 ppm), Al (85 ppm), Si (87 ppm), Ti (128 ppm), Mn (774 ppm), Ca (152 ppm), Fe (562 ppm), Y (270 ppm), La (1682 ppm), Ce (1517 ppm), Th (690 ppm), and U (938 ppm). Analytical accuracy for garnet and epidote was monitored by employing the following standards: GRTPYR, GRTGM, CPX511, ilmenite, Cr metal, bustamite, and hematite for garnet, whereas bytownite, bustamite, olivine, ilmenite, hematite, CPX511, U metal, Th metal, PhosCe, PhosLa, and Yag were analyzed for epidote. The concentrations of the elements analyzed in each mineral were converted to molar cation numbers standardized to the appropriate number of oxygen atoms in the mineral.

4. Results and discussion

4.1. Garnet

Electron probe microanalyses (EPMA) show that garnets from the MG skarn deposits mostly belong to the grossular–andradite (grandite) solid solution. Generally, crystal compositions vary from $Adr_{16}Gr_{82}$ to almost pure andradite – $Adr_{99}Gr_1$ (Fig. 5a; Table 1), with spessartine, pyrope, uvarovite, and almandine, collectively less than 5%. All these garnet varieties are part of the solid solution of skarn garnets and do not represent separate garnet stages within the deposit. Garnet formula unit and end-members were calculated based on 12 oxygens and with Fe^{2+}/Fe^{3+} calculated assuming full site occupancy. Garnet from prograde skarn has high Al_2O_3 contents ranging from 13.78 to 17.47 wt% (average 15.77 wt%) compared to retrograde garnet, which exhibits low Al_2O_3 values ranging from 0.24 to 14.76 wt% (average 6.90 wt%). Prograde garnet is low in total iron, i.e. FeO^T (6.84–11.89 wt%; average 9.04 wt%) compared to retrograde garnets that have FeO^T contents ranging from 10.45 to 27.92 wt% (average 19.71 wt%). Hornfels contains the highest FeO^T (22.32–27.18 wt%; average 23.42 wt%) and the lowest Al_2O_3 (1.43–5.53 wt%; average 4.62 wt%) values. High FeO in hornfels is attributed to the presence of magnetite that occur as massive and/or dissemination and cannot be avoided during EPMA analysis. These prograde/early garnets are commonly zoned with grandite cores and andraditic rims, which are typical of garnets in porphyry-related copper skarns (e.g., Einaudi, 1982). The variation in garnet composition from core to rim coupled with oscillatory zoning may reflect physico-chemical changes, such as those that would be produced by cyclic hydraulic fracturing or *syn*-tectonic mineralization.

4.2. Pyroxene

Clinopyroxene from the MG skarn deposit forms a solid solution series between diopside and hedenbergite with a composition from hedenbergitic or ferroan diopside – $Di_{31}Hd_{60}$ to diopsidic – $Di_{93}Hd_7$) (Fig. 5b; Table 2), whereas other pyroxene compositions collectively account for less than 10% of the pyroxenes. Like the garnets, the pyroxenes exhibit an intracrystalline chemical zonation, with diopsidic cores and hedenbergitic or ferroan diopside rims. Pyroxene also exhibits a wide compositional range from prograde to retrograde stage. This pyroxene from prograde skarn is Mg-rich with MgO ranging from 13.07 to 17.38 wt% (average 15.85 wt%), whereas retrograde pyroxene exhibits lower MgO and ranges from 7.05 to 11.78 wt% (average 9.60 wt %). In terms of FeO content pyroxene from prograde skarn is low (FeO 1.34–7.42 wt%, average 3.11 wt%) compared to retrograde pyroxene where FeO ranges from 9.95 to 16.73 wt% (average 12.98 wt%). Iron enrichment in pyroxene from prograde to retrograde is a result of continuous substitution of Mg with Fe as the hydrothermal system evolves (Fig. 6c). Similar to garnet, pyroxene from the hornfels zone contains the highest FeO (14.49–25.38 wt%; average 19.45 wt% FeO and lowest MgO (0.07–8.49 wt%; average = 4.91 MgO wt%) values possibly due to Fe-metasomatism.

4.3. Wollastonite, amphibole, vesuvianite, and epidote

Wollastonite in the MG skarn occurs sporadically as a minor constituent in massive pyroxene in areas proximal to dyke contacts and/or in endoskarn. It is close to its stoichiometric composition ($CaSiO_3$), with minor amounts of Fe, Al, Mg, Mn, and Na oxides (Table 3). According to classification by Leake et al. (2004), calcic-amphiboles in the MG skarn system (Table 4) belong to magnesio-hornblende, ferro-tschermakite, and actinolite with the dominant substitution being among Fe, Mg and Mn in the M1-M3 with minimal or no substitution for Ca due to full occupancy of the M4 site (Fig. 6b). Most of the amphibole occurs as retrograde alteration product of pyroxene, typically in association with quartz, carbonate, and sulfides. Other phases include minor vesuvianite that occurs sporadically and contains significant amounts of Mg, Al, and Fe oxides (Table 5). Epidote occurs most commonly in veins and veinlets
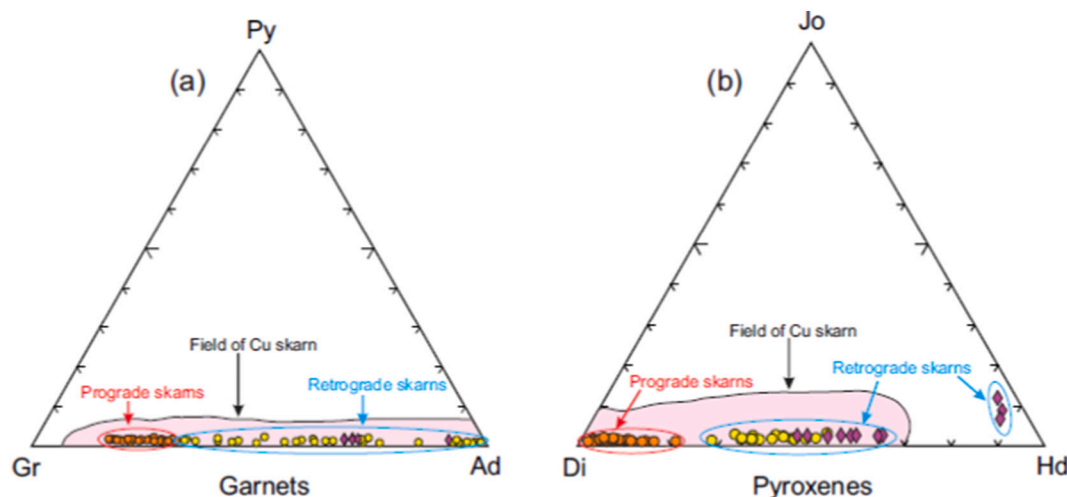
Fig. 5. Compositions of calc-silicates from the McKenzie Gulch skarn occurrences; plots of garnet compositions (a) in grossular – (pyrope + almandine + spessartine) – andradite diagram; (b) clinopyroxene composition in diopside–hedenbergite–johannsenite diagram. Compositional fields for garnets and pyroxenes for Cu-dominated skarns are from Meinert (1983). Hornfels samples fall in the retrograde field possibly due to contamination by Fe present in magnetite associated with hornfels. Symbols as in Fig. 6 below.

Table 1
Composition of garnet from McKenzie Gulch skarns as determined by EPMA.

Rock type	Skarn	Skarn	Skarn	Skarn	Skarn	Skarn	Skarn	Skarn	Skarn
Sample	Mc-92-19a	Mc-92-19a	Mc-92-19a	Mc-92-19a	Mc-92-19a	Mc-92-19a	Mc-92-19a	Mc-92-19a	Mc-92-19a
Analytical spot	1	2	3	4	5	6	7	8	9
Comments	Prog	Prog	Prog	Prog	Prog	Prog	Prog	Prog	Prog
Oxide weight %									
SiO_2	38.49	38.55	38.37	38.70	39.11	38.82	38.58	38.26	38.87
TiO_2	0.48	0.46	0.48	0.43	0.32	0.11	0.65	0.50	0.34
Al_2O_3	15.08	15.15	14.46	15.57	17.47	17.43	16.09	13.78	16.81
FeO	9.34	9.07	10.02	8.66	6.84	8.33	9.12	10.53	7.46
MnO	0.24	0.21	0.21	0.19	0.24	0.58	0.54	0.22	0.28
MgO	0.29	0.27	0.31	0.27	0.25	0.11	0.13	0.30	0.24
CaO	34.90	34.86	34.89	35.00	35.08	33.77	33.81	34.76	34.99
Cr_2O_3	0.01	0.00	0.01	0.00	0.01	0.00	0.01	0.00	0.00
Total	**98.83**	**98.57**	**98.74**	**98.82**	**99.33**	**99.14**	**98.93**	**98.36**	**99.00**
Corrected oxide percentages based on 12 oxygens and with Fe^{2+}/Fe^{3+} calculated assuming full site occupancy									
SiO_2	38.49	38.55	38.37	38.70	39.11	38.82	38.58	38.26	38.87
TiO_2	0.48	0.46	0.48	0.43	0.32	0.11	0.65	0.50	0.34
Al_2O_3	15.08	15.15	14.46	15.57	17.47	17.43	16.09	13.78	16.81
Cr_2O_3	0.01	0.00	0.01	0.00	0.01	0.00	0.01	0.00	0.00
Fe_2O_3	7.91	7.69	8.61	7.30	5.32	5.40	6.54	9.20	6.01
FeO	2.22	2.15	2.27	2.09	2.05	3.47	3.24	2.25	2.05
MnO	0.24	0.21	0.21	0.19	0.24	0.58	0.54	0.22	0.28
MgO	0.29	0.27	0.31	0.27	0.25	0.11	0.13	0.30	0.24
CaO	34.90	34.86	34.89	35.00	35.08	33.77	33.81	34.76	34.99
Total	**99.62**	**99.34**	**99.60**	**99.55**	**99.86**	**99.69**	**99.59**	**99.28**	**99.60**
Number of ions based on 12 oxygen atoms and end-member calculation									
Si	3.015	3.024	3.016	3.023	3.018	3.016	3.015	3.025	3.018
Al^{iv}	0.000	0.000	0.000	0.000	0.000	0.000	0.000	0.000	0.000
Al^{vi}	1.420	1.428	1.369	1.460	1.610	1.617	1.506	1.314	1.561
Ti	0.028	0.027	0.028	0.025	0.018	0.006	0.038	0.030	0.020
Cr	0.001	0.000	0.000	0.000	0.001	0.000	0.000	0.000	0.000
Fe^{3+}	0.466	0.454	0.510	0.429	0.309	0.316	0.384	0.548	0.351
Fe^{2+}	0.146	0.141	0.149	0.137	0.133	0.226	0.212	0.149	0.133
Mn	0.016	0.014	0.014	0.013	0.016	0.038	0.036	0.015	0.019
Mg	0.033	0.032	0.036	0.031	0.029	0.012	0.015	0.036	0.028
Ca	2.929	2.930	2.938	2.929	2.901	2.811	2.831	2.944	2.911
Total	**8.054**	**8.049**	**8.060**	**8.047**	**8.034**	**8.043**	**8.038**	**8.060**	**8.041**
Almandine	0.0	0.0	0.0	0.0	0.0	0.2	0.0	0.0	0.0
Andradite	25.1	24.5	27.5	23.0	16.3	16.5	20.6	29.9	18.6
Grossular	73.1	73.9	70.6	75.4	82.1	81.5	77.6	68.3	79.8
Pyrope	1.2	1.1	1.3	1.1	1.0	0.4	0.5	1.3	1.0
Spessartine	0.6	0.5	0.5	0.5	0.6	1.3	1.3	0.5	0.7
Uvarovite	0.0	0.0	0.0	0.0	0.0	0.0	0.0	0.0	0.0
Total	**100.0**	**100.0**	**100.0**	**100.0**	**100.0**	**100.0**	**100.0**	**100.0**	**100.0**

in association with amphibole, calcite, quartz, and sulfides. Epidote (EP) from MG contains clinozoisite component and ranges from EP15 to nearly pure-EP31 Fe-end-member (Table 6, Fig. 6d). The epidote commonly exhibits zoning, i.e. Fe-enrichment toward crystal rims, although reverse zoning does occur due to physico-chemical variations of the fluids. Sulfide minerals are commonly associated with this type of alteration in addition to amphiboles, quartz, and calcite.

4.4. Skarn formation and alteration

The MG deposit consists mainly of exoskarn with minor endoskarn zones. The latter commonly occur at the margins of porphyry dykes where they formed as discordant veins and/or irregular pods. The presence of numerous dykes in the study area complicates the alteration patterns of the MG skarn system relative to other skarn deposits (Fig. 7). For example, a 200-m-long horizontal drill hole oriented N70W (perpendicular to the dike swarm) intersected eight intervals of porphyry dykes (1–3 m wide) and nine zones of skarn (1 m wide) within argillaceous limestones. The percentage volume of dykes intrusion within skarn alteration and mineralization zones is estimated to be between 30 and 40%. Although an estimated mineralization occurs within

a 10 m thick envelop, skarn alteration is widespread and it varies from 50 m to 100 m thick on surface, and extends down to a depth of about 500 m. Other small and sporadic patches of mineralized and barren skarn alteration zones do occur in the study area. These endoskarn alteration zones mainly consist of pale brown to colorless, medium- to coarse-grained garnet and pyroxene, chlorite, calcite, sericite, quartz, and pseudomorphs of the primary feldspar (Fig. 3).

Exoskarn zones developed as a result of metamorphism that converted the argillaceous limestone into a fine-grained calc-silicate marble that contains prograde assemblages of andradite and grossularite-rich garnet (Fig. 3), diopsidic to hedenbergitic clinopyroxene, wollastonite, vesuvianite, calcite, quartz, plagioclase and titanite, and the calcareous mudstone into fine-grained calc-silicate hornfels (Fig. 3). These prograde skarn assemblages occur as (1) complete replacement of the primary bedding textures, (2) thin reaction bands between argillaceous limestone and calc-silicate hornfels layers (Fig. 3), or (3) thin millimeter to centimeter thick veins cutting across alternating layers of calc-silicate hornfels and skarns. The retrograde alteration developed in the late stages of skarn development and affects the previously metamorphosed and metasomatized lithological units and the intruding felsic porphyry dykes. This retrograde alteration overprint both hornfels and skarns

Table 2
Composition of pyroxene from McKenzie Gulch skarns as determined by EPMA.

Rock type	Skarn	Skarn	Skarn	Skarn	Skarn	Skarn	Skarn	Skarn	Skarn	Skarn	Skarn
Sample	MC-92-19A	MC-92-19A	MC-92-19A	MC-92-19A	MC-92-19A	MC-92-19A	MC-92-19A	MC-92-19A	MC-92-19A	MC-92-19A	MC-92-19A
Analytical spot	1	2	3	4	5	6	7	8	9	10	11
Comments	Prog	Prog	Prog	Prog	Prog	Prog	Prog	Prog	Prog	Prog	Prog
Oxide weight %											
SiO_2	51.55	53.59	53.88	54.11	52.03	53.84	52.52	54.32	53.86	52.79	53.69
TiO_2	0.01	0.00	0.02	0.05	0.02	0.00	0.01	0.01	0.15	0.00	0.02
Al_2O_3	0.27	0.34	0.40	0.52	1.80	0.40	1.06	0.69	1.22	3.74	0.52
FeO	1.76	4.36	2.26	1.56	4.70	3.13	4.12	1.45	2.55	2.06	3.62
MnO	0.24	0.21	0.19	0.05	0.21	0.25	0.24	0.03	0.05	0.27	0.30
MgO	16.24	15.26	16.38	16.82	14.52	15.78	15.10	16.98	16.00	14.13	15.62
CaO	24.98	25.51	25.76	25.69	25.56	25.81	25.92	25.64	25.04	25.78	25.82
Na_2O	0.10	0.16	0.17	0.17	0.08	0.13	0.03	0.18	0.41	0.10	0.08
Cr_2O_3	0.03	0.01	0.03	0.01	0.01	0.02	0.00	0.00	0.01	0.01	0.00
K_2O	0.01	0.01	0.00	0.01	0.00	0.00	0.01	0.01	0.00	0.00	0.01
Total	**95.18**	**99.44**	**99.09**	**98.99**	**98.93**	**99.37**	**99.01**	**99.31**	**99.3**	**98.88**	**99.67**
Number of ions based on 6 oxygen atoms											
Si	1.971	1.976	1.976	1.978	1.937	1.977	1.950	1.976	1.965	1.934	1.973
Ti	0.000	0.000	0.000	0.000	0.000	0.000	0.000	0.000	0.004	0.000	0.000
Al	0.012	0.015	0.017	0.023	0.080	0.017	0.047	0.030	0.053	0.164	0.023
Fe	0.057	0.136	0.070	0.048	0.148	0.097	0.130	0.045	0.079	0.064	0.113
Mn	0.008	0.007	0.006	0.000	0.007	0.008	0.008	0.000	0.000	0.008	0.009
Mg	0.938	0.850	0.907	0.929	0.817	0.875	0.847	0.933	0.882	0.782	0.867
Ca	1.037	1.021	1.026	1.020	1.034	1.029	1.045	1.013	0.992	1.025	1.030
Na	0.000	0.023	0.025	0.024	0.000	0.019	0.000	0.025	0.059	0.015	0.000
Cr	0.000	0.000	0.000	0.000	0.000	0.000	0.000	0.000	0.000	0.000	0.000
K	0.000	0.000	0.000	0.000	0.000	0.000	0.000	0.000	0.000	0.000	0.000
Total cations	**4.023**	**4.028**	**4.028**	**4.023**	**4.023**	**4.023**	**4.026**	**4.022**	**4.034**	**3.992**	**4.016**
Wo (%)	52.51	51.79	52.02	51.52	53.13	52.06	53.21	51.25	51.27	52.94	52.06
En (%)	47.49	43.11	46.02	46.94	41.99	44.29	43.13	47.23	45.58	40.37	43.82
Fs (%)	0.00	5.10	1.96	1.54	4.88	3.66	3.65	1.52	3.15	6.69	4.12
CPX Group	Ca-Mg-Fe	Ca-Mg-Fe	Ca-Mg-Fe	Ca-Mg-Fe	Ca-Mg-Fe	Ca-Mg-Fe	Ca-Mg-Fe	Ca-Mg-Fe	Ca-Mg-Fe	Ca-Mg-Fe	Ca-Mg-Fe
CPX Name	Di	Di	Di	Di	Di	Di	Di	Di	Di	Di	Di

Notes: Wo = wollastonite, En = Enstatite, Di = Diopside, Hd = Hedenbergite, Fs = Ferrosilite, CPX = clinopyroxene, H/fels = hornfels, Retro = retrograde.

either completely or partially. The overprinting relationships indicate that alteration facies formed during a complex prograde-retrograde alteration sequence, which resulted from multiple episodes of magma injection as shallow dykes (see Massawe and Lentz, 2019, 2020). These stages are recorded in the rock as a series of crosscutting features and interesting alteration textures and/or patterns that reflect a skarn and associated magmatic-hydrothermal ore deposits worldwide (Einaudi et al., 1981; Bendezú and Fontboté, 2002; Rusk and Reed, 2002; Meinert et al., 2003).

4.5. Mineralization and lithological control

Copper–silver skarn mineralization at the MG area is commonly associated with retrograde alteration assemblages suggesting that sulfide precipitation did not take place until the system was diluted by fluids with lower salinities and cooled below the temperature of early stage skarn formation (Massawe and Lentz, 2021). This mineralization is principally hosted within the Matapédia Group that consists of thin-bedded, dark grey argillaceous limestone and calcareous siltstone (Lentz et al., 1995; Fig. 3). In the MG area skarn contains between 3 and 15% total sulfides and minor oxides, whereas the hornfels zone may contain 0–15% magnetite, locally reflecting a major Fe-metasomatism during hornfels formation. In some cases magnetite is retrograde as it replaces garnet and occurs in association with pyrite and chalcopyrite (Fig. 3E), which suggests reduction of hydrothermal fluids at least locally as they interact with carbon-bearing rocks (commonly argillaceous limestone).

Sulfide minerals overprint all skarn assemblages. Pyrrhotite and chalcopyrite are most dominant and together they comprise about 3–10% of all sulfides, whereas pyrite constitutes 1–5%. This assemblage of sulfides suggests a reduced oxidation state of retrograde fluids. These sulfides occur most commonly as veins or a stockwork of veinlets, or as disseminated, patchy and locally as replacement bodies within calc-silicate skarn in argillaceous limestone (Fig. 3). Minor late sphalerite is associated with pyrite or pyrrhotite and occurs within endoskarn veins, proximal to intrusive contacts or cross cutting skarn or hornfels (Fig. 3O). Metalliferous skarns associated with the MG occurrences are Cu-rich and contain significant amounts of Ag. In addition, gold-bearing quartz-sulfide veins adjacent to skarn deposit (Fig. 3A), are up to 50 cm wide with the majority ranging between 5 and 25 cm. The sulfides phases in these veins are dominated by pyrrhotite, chalcopyrite, and pyrite, with subordinate sphalerite and galena. The exposed hypogene skarn and Au-bearing sulfides in the MG area were locally subjected to supergene processes which replaced primary sulfide minerals by oxides and hydroxides of iron, and copper carbonates, to form small leached caps and patches as oxide zones (Fig. 3B). Fig. 8 presents the paragenetic sequence of minerals from the skarn and oxide zones. This sequence was established based on the data from geological mapping, drill core logging, and petrographic examination. The spatially and temporally associated dykes in the MG area are generally unmineralized except locally where they are in contact with skarn. However, dykes emplacement and skarn mineralization was contemporaneous and it occurred during the Middle Devonian (Massawe and Lentz, 2019, 2020).

5. Conclusions

1. The MG deposit is a small size and calcic and mildly oxidized skarn deposit hosted by calcareous sedimentary rocks of the Matapédia
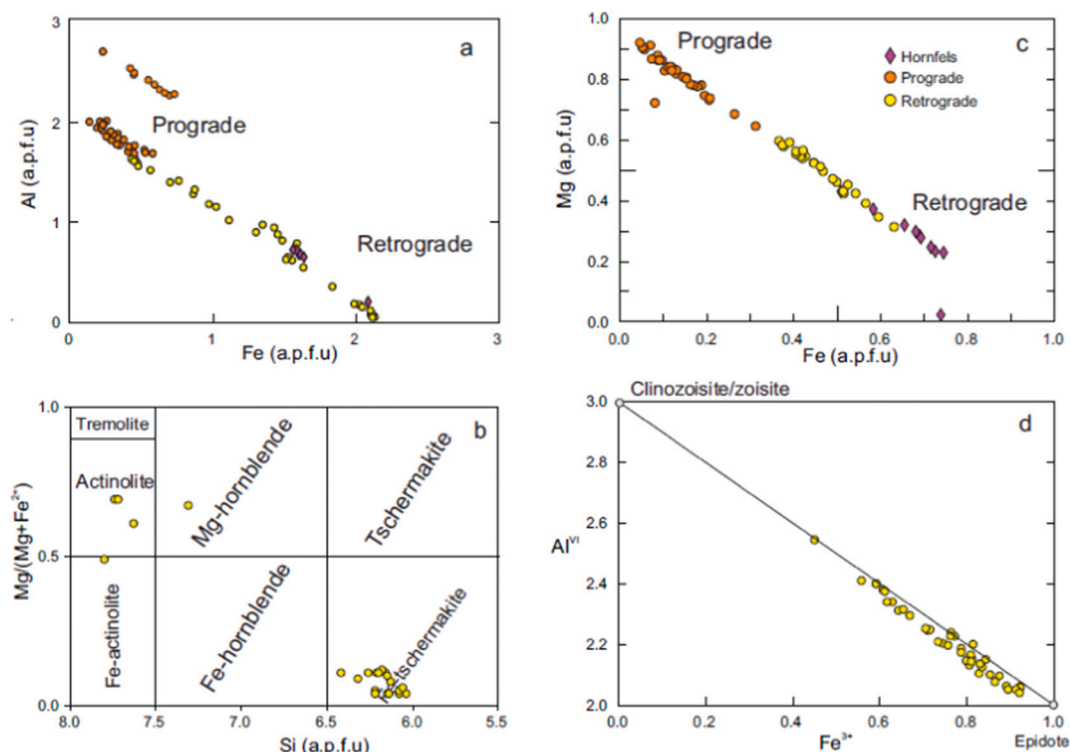
Fig. 6. Compositions of calc-silicates from the McKenzie Gulch skarn occurrences; plots of garnet compositions (a) in Al (a.p.f.u) versus Fe (a.p.f.u) diagram; (b) amphibole composition in $Mg/(Mg + Fe^{2+})$ vs Si (a.p.f.u) diagram (Leake et al., 2004); and (c) pyroxene in Mg (a.p.f.u) versus Fe (a.p.f.u) diagram; (d) distribution of octahedral Al and Fe^{3+} for epidotes from the MG skarn samples (Armbruster et al., 2006). Abbreviation: a.p.f.u. = atom per formula unit.

Table 3
Composition of wollastonite from McKenzie Gulch skarns as determined by EPMA.

Rock type	Skarn	Skarn	Skarn	Skarn	Skarn	Skarn	Skarn	Skarn
Sample	97-DL-125A	97-DL-125A	97-DL-125A	97-DL-125A	97-DL-125A	97-DL-125A	97-DL-125A	97-DL-125A
Analytical spot	58	59	60	68	69	73	74	75
Comments	Prog	Prog	Prog	Prog	Prog	Prog	Prog	Prog
Oxide weight %								
SiO_2	51.47	51.29	51.30	50.68	51.07	51.25	51.56	51.45
TiO_2	0.00	0.01	0.00	0.00	0.00	0.00	0.00	0.01
Al_2O_3	0.07	0.06	0.11	0.01	0.05	0.19	0.03	0.05
FeO	0.42	0.42	0.50	0.41	0.43	0.44	0.25	0.40
MnO	0.16	0.17	0.21	0.16	0.18	0.19	0.17	0.17
MgO	0.08	0.09	0.10	0.06	0.09	0.05	0.08	0.22
CaO	48.15	48.41	48.29	47.49	48.29	48.14	48.45	48.03
Na_2O	0.00	0.01	0.00	0.01	0.07	0.02	0.00	0.01
Cr_2O_3	0.00	0.00	0.00	0.00	0.00	0.00	0.01	0.00
K_2O	0.01	0.01	0.01	0.01	0.04	0.00	0.00	0.00
Total	**100.38**	**100.46**	**100.53**	**98.84**	**100.22**	**100.29**	**100.55**	**100.36**
Number of ions based on 6 oxygen atoms								
Si	1.983	1.977	1.975	1.982	1.976	1.975	1.982	1.980
Ti	0.000	0.000	0.000	0.000	0.000	0.000	0.000	0.000
Al	0.000	0.000	0.005	0.000	0.000	0.009	0.000	0.000
Fe	0.014	0.014	0.016	0.014	0.014	0.014	0.008	0.013
Mn	0.005	0.006	0.007	0.005	0.006	0.006	0.006	0.006
Mg	0.000	0.000	0.000	0.000	0.000	0.000	0.000	0.013
Ca	2.015	2.027	2.019	2.017	2.029	2.015	2.022	2.008
Na	0.000	0.000	0.000	0.000	0.000	0.000	0.000	0.000
K	0.000	0.000	0.000	0.000	0.000	0.000	0.000	0.000
Total cations	**4.017**	**4.023**	**4.022**	**4.018**	**4.024**	**4.020**	**4.018**	**4.020**
CPX Group	Ca-Si	Ca-Si	Ca-Si	Ca-Si	Ca-Si	Ca-Si	Ca-Si	Ca-Si
CPX Name	Wo	Wo	Wo	Wo	Wo	Wo	Wo	Wo

Table 4
Composition of amphibole from McKenzie Gulch skarns as determined by EPMA.

Rock type	Skarn	Skarn	Skarn	Skarn	Skarn	Skarn	Skarn	Skarn	Skarn	Skarn	Skarn	Skarn
Sample	97-DL-116	97-DL-116	97-DL-116	97-DL-116	97-DL-116	97-DL-116	97-DL-116	97-DL-116	97-DL-116	97-DL-116	97-DL-116	97-DL-116
Analytical spot	11	12	13	14	15	16	17	18	19	20	21	22
Comments	Retro	Retro	Retro	Retro	Retro	Retro	Retro	Retro	Retro	Retro	Retro	Retro
Oxide weight %												
SiO_2	37.16	37.78	38.29	37.67	38.07	37.79	38.78	37.25	36.66	38.52	38.25	37.47
TiO_2	0.38	0.32	0.49	0.43	0.54	0.17	0.55	0.62	0.46	0.24	0.46	0.43
Al_2O_3	11.26	12.05	11.00	11.79	10.62	11.39	11.54	12.10	11.81	10.32	11.71	10.60
FeO	32.34	29.99	30.11	29.04	33.09	32.38	30.70	32.74	32.09	31.11	30.06	32.75
MnO	0.19	0.18	0.19	0.19	0.25	0.23	0.21	0.19	0.23	0.24	0.20	0.23
MgO	0.84	1.99	2.04	2.27	0.97	1.57	2.05	0.81	0.79	1.74	2.09	0.76
CaO	11.25	11.25	11.23	11.25	11.23	11.69	11.65	11.59	11.15	11.39	11.31	11.02
K_2O	2.00	2.03	2.21	2.13	1.99	2.37	2.00	1.85	1.85	2.15	2.23	2.05
Na_2O	1.48	1.42	1.23	1.28	1.49	1.29	1.39	1.74	1.67	1.25	1.30	1.50
Cr_2O_3	0.00	0.00	0.00	0.00	0.00	0.00	0.00	0.00	0.02	0.01	0.01	0.01
BaO	0.03	0.09	0.00	0.00	0.09	0.00	0.00	0.02	0.05	0.00	0.03	0.00
F	0.36	0.29	0.29	0.28	0.32	0.26	0.32	0.35	0.33	0.29	0.30	0.31
Cl	1.43	1.05	1.20	0.95	1.59	1.96	1.27	1.34	1.37	1.50	1.15	1.62
Total	**98.71**	**98.44**	**98.29**	**97.28**	**100.26**	**101.09**	**100.45**	**100.60**	**98.47**	**98.75**	**99.10**	**98.75**
Number of ions based on 23 oxygen atoms												
Si	6.154	6.157	6.262	6.180	6.224	6.132	6.208	6.044	6.078	6.324	6.196	6.224
Ti	0.048	0.039	0.061	0.054	0.068	0.021	0.067	0.077	0.059	0.030	0.057	0.055
Al	2.228	2.346	2.149	2.311	2.074	2.208	2.207	2.345	2.339	2.024	2.266	2.103
Fe	4.580	4.142	4.173	4.038	4.586	4.453	4.166	4.502	4.510	4.329	4.127	4.611
Mn	0.027	0.025	0.027	0.027	0.035	0.032	0.028	0.026	0.032	0.033	0.028	0.033
Mg	0.210	0.490	0.505	0.562	0.240	0.385	0.496	0.200	0.198	0.431	0.511	0.191
Ca	2.023	1.991	1.994	2.004	1.994	2.060	2.025	2.042	2.008	2.031	1.989	1.988
K	0.428	0.427	0.467	0.451	0.422	0.497	0.414	0.388	0.396	0.458	0.467	0.440
Na	0.480	0.456	0.396	0.413	0.480	0.410	0.436	0.553	0.543	0.404	0.414	0.490
Cr	0.000	0.000	0.000	0.000	0.000	0.000	0.000	0.000	0.000	0.000	0.000	0.000
Ba	0.000	0.000	0.000	0.000	0.000	0.000	0.000	0.000	0.000	0.000	0.000	0.000

Table 5
Composition of vesuvianite from McKenzie Gulch skarns as determined by EPMA.

Rock type	Skarn	Skarn	Skarn	Skarn	Skarn	Skarn	Skarn	Skarn	Skarn	Skarn
Sample	97-DL-100	97-DL-100	97-DL-100	97-DL-100	97-DL-100	97-DL-100	97-DL-100	97-DL-100	97-DL-100	97-DL-100
Analytical spot	1	2	3	4	5	6	7	8	9	10
Oxide weight %										
K_2O	0.00	0.01	0.00	0.01	0.00	0.00	0.00	0.00	0.01	0.00
Cr_2O_3	0.00	0.01	0.01	0.00	0.00	0.00	0.04	0.01	0.00	0.00
Na_2O	0.03	0.00	0.01	0.17	0.09	0.02	0.18	0.14	0.03	0.12
SiO_2	36.94	36.88	36.71	37.14	37.30	37.05	37.33	37.31	37.02	37.31
MnO	0.05	0.07	0.10	0.09	0.08	0.08	0.08	0.10	0.08	0.08
CaO	36.70	36.68	36.29	36.09	36.70	36.69	36.01	36.76	36.89	36.85
TiO_2	1.91	0.64	1.21	2.80	1.20	1.59	1.57	1.75	2.11	1.94
MgO	2.82	2.97	3.04	1.83	1.90	2.85	1.87	2.13	2.81	2.29
Al_2O_3	15.76	15.48	15.31	16.97	17.78	15.95	17.13	16.65	15.60	16.48
FeO	3.26	4.49	4.27	2.68	2.95	3.39	3.37	3.38	3.36	3.05
BaO	0.02	0.00	0.00	0.00	0.00	0.00	0.00	0.02	0.08	0.05
F	1.04	0.95	0.84	1.19	1.40	1.05	1.16	1.33	0.93	1.41
Cl	0.51	0.19	0.52	0.47	0.22	0.21	0.21	0.14	0.28	0.16
Total	**99.05**	**98.37**	**98.31**	**99.43**	**99.62**	**98.87**	**98.95**	**99.72**	**99.19**	**99.75**
Mole cations										
K	0.000	0.000	0.000	0.000	0.000	0.000	0.000	0.000	0.000	0.000
Cr	0.000	0.000	0.000	0.000	0.000	0.000	0.000	0.000	0.000	0.000
Na	0.000	0.000	0.000	0.082	0.000	0.000	0.086	0.067	0.000	0.061
Si	9.240	9.305	9.281	9.203	9.233	9.255	9.289	9.246	9.233	9.249
Mn	0.000	0.000	0.000	0.000	0.000	0.000	0.000	0.022	0.000	0.000
Ca	9.969	10.050	9.963	9.712	9.865	9.953	9.730	9.892	9.991	9.920
Ti	0.365	0.123	0.232	0.528	0.227	0.303	0.298	0.331	0.401	0.366
Mg	1.065	1.133	1.161	0.686	0.710	1.074	0.704	0.796	1.060	0.859
Al	4.709	4.666	4.624	5.023	5.258	4.760	5.092	4.929	4.648	4.880
Fe	0.691	0.960	0.915	0.562	0.618	0.718	0.711	0.710	0.710	0.641
Ba	0.000	0.000	0.000	0.000	0.000	0.000	0.000	0.000	0.000	0.000

Table 6

Composition of epidote from McKenzie Gulch skarns as determined by EPMA.

Rock type	Skarn	Skarn	Skarn	Skarn	Skarn	Skarn	Skarn	Skarn	Skarn	Skarn	Skarn	Skarn
Sample	97-DL-140	97-DL-140	97-DL-140	97-DL-140	97-DL-140	97-DL-140	97-DL-140	97-DL-140	97-DL-140	97-DL-140	97-DL-140	97-DL-140
Analytical spot	1	2	3	4	5	6	7	8	9	10	11	12
Comments	–	–	–	–	–	–	–	–	–	–	–	–
Oxide weight %												
SiO_2	38.23	38.79	39.00	38.56	38.50	38.11	37.56	38.30	38.69	38.03	38.50	38.48
MnO	0.20	0.05	0.05	0.04	0.16	0.03	0.05	0.03	0.06	0.03	0.02	0.15
CaO	23.30	23.53	23.76	23.39	22.89	24.26	23.77	23.83	23.97	23.67	24.03	23.35
TiO_2	0.12	0.11	0.08	0.05	0.05	0.08	0.04	0.34	0.10	0.06	0.10	0.02
MgO	0.03	0.04	0.02	0.03	0.07	0.03	0.03	0.06	0.04	0.05	0.06	0.05
Al_2O_3	23.51	25.07	25.58	23.22	24.06	25.81	21.98	22.67	25.45	22.76	24.91	23.30
FeO	11.91	9.80	9.67	12.33	11.73	9.27	13.83	12.55	9.43	12.57	10.21	12.85
Y_2O_3	0.00	0.00	0.00	0.00	0.00	0.00	0.00	0.00	0.00	0.00	0.00	0.00
La_2O_3	0.00	0.00	0.05	0.02	0.00	0.01	0.01	0.05	0.00	0.00	0.08	0.14
Ce_2O_3	0.02	0.13	0.00	0.00	0.00	0.12	0.08	0.02	0.03	0.00	0.00	0.00
ThO_2	0.00	0.04	0.00	0.00	0.02	0.01	0.00	0.02	0.02	0.01	0.05	0.01
UO_2	0.00	0.03	0.05	0.04	0.02	0.00	0.00	0.00	0.03	0.01	0.06	0.00
Total	97.33	97.59	98.27	97.68	97.51	97.73	97.36	97.88	97.83	97.19	98.01	98.33
Number of ions based on 12.5 oxygen atoms												
Si	3.018	3.037	3.028	3.034	3.025	2.984	2.991	3.019	3.020	3.016	3.011	3.015
Ti	0.007	0.006	0.005	0.003	0.003	0.005	0.002	0.020	0.006	0.003	0.006	0.001
Al^{VI}	2.188	2.313	2.341	2.153	2.228	2.381	2.063	2.106	2.341	2.127	2.296	2.152
Fe^{3+}	0.786	0.642	0.628	0.811	0.771	0.607	0.921	0.827	0.616	0.834	0.668	0.842
Mn	0.013	0.003	0.003	0.003	0.011	0.002	0.004	0.002	0.004	0.002	0.001	0.010
Mg	0.004	0.004	0.002	0.004	0.008	0.004	0.004	0.007	0.005	0.006	0.006	0.006
Ca	1.971	1.974	1.976	1.972	1.927	2.035	2.028	2.013	2.005	2.011	2.013	1.960
Na	0.000	0.000	0.000	0.000	0.000	0.000	0.000	0.000	0.000	0.000	0.000	0.000
K	0.000	0.000	0.000	0.000	0.000	0.000	0.000	0.000	0.000	0.000	0.000	0.000
H	1.000	1.000	1.000	1.000	1.000	1.000	1.000	1.000	1.000	1.000	1.000	1.000
EP (%)	26.442	21.715	21.151	27.368	25.703	20.310	30.867	28.204	20.819	28.156	22.532	28.127

Notes: EP – Clinozoisite component in epidote = $(Fe^{3+}/(Fe^{3+}+Al)^{VI} *100$, Retro = retrograde, Prog = prograde, trans = transitional; FeO = total iron.
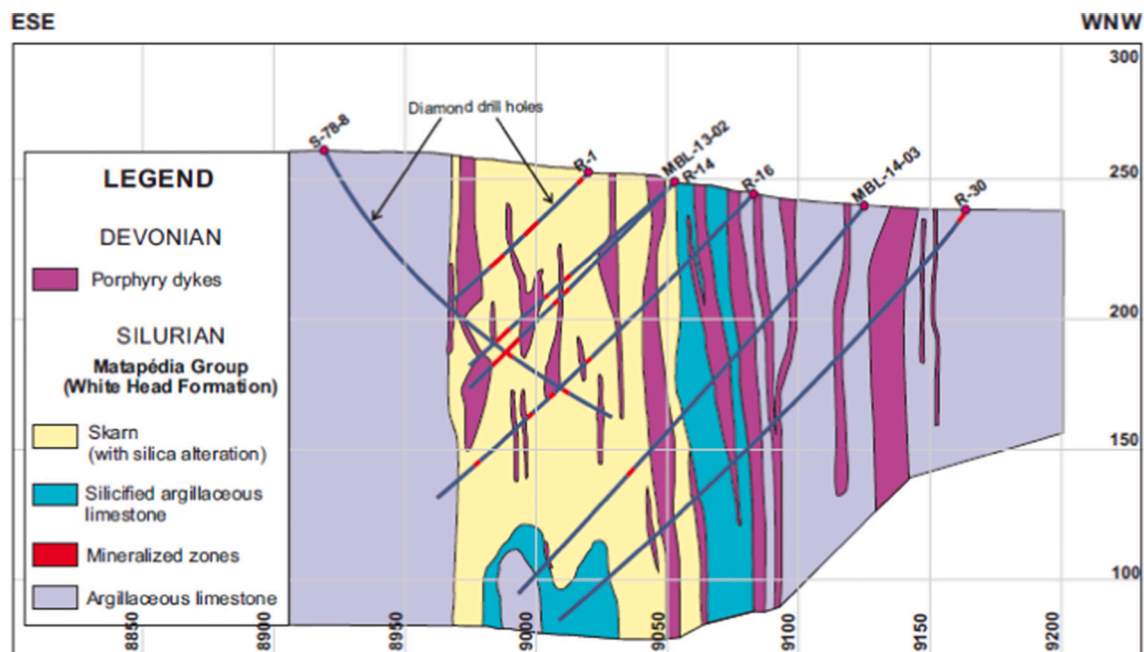

Fig. 7. A cross section through one of the McKenzie Gulch Cu—Ag skarn mineralized zones (modified from Desrosier, 2013).

Group. The host rocks, style of mineralization and the regional geology of this area are similar to those in the southern Gaspé, Québec (see Malo et al., 2000). By analogy the Cu—Ag skarn and related Au-bearing quartz vein occurrences at the MG are explained by a similar intrusion-related hydrothermal model. This model opens the possibility for porphyry-related sulfide and/or Au exploration in the northwestern New Brunswick and Gaspé Peninsula.
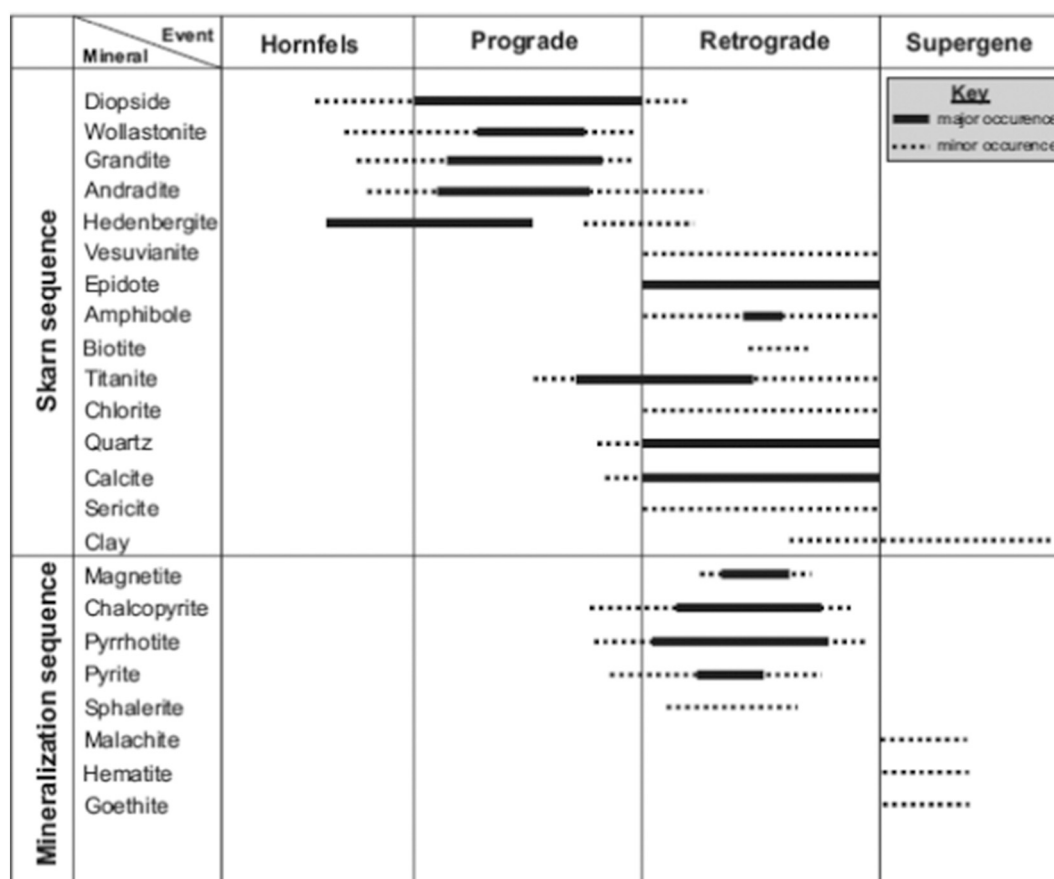
Fig. 8. Paragenetic sequence diagram for skarn and ore minerals from the MG occurrences and adjacent Au–bearing quartz–sulfide veins. Evidence used for the paragenetic relation includes micro- and macro-textural data (i.e. field & drill core observations, microscopic examination, and EPMA results).

2. Detailed petrographic examination and major element geochemistry of calc-silicates from MG skarns suggest that early prograde skarn conditions were chemically buffered by bulk rock compositions in a relatively low water/rock ratio environment to form grandite-diopside, but evolved to higher water/rock ratio conditions that introduced large amounts of iron during later stages of the prograde skarn event. This transition is recorded in the chemical zonation within individual garnets and pyroxenes."

3. Data from mineral chemistry suggest that there is a close ties between the composition of pyroxene and garnet within the skarn and the dominant metal (i.e. copper in this case) and thus this relationships can be used as an exploration tool during exploration for porphyry Cu and skarn as well as related magmatic-hydrothermal ore deposits.

CRediT authorship contribution statement

Ronald J. Massawe: Conceptualization, Methodology, Software, Data curation, Writing – original draft, Visualization, Investigation, Software, Validation, Writing – review & editing. **David R. Lentz:** Conceptualization, Funding acquisition, Project administration, Supervision, Writing – review & editing.

Declaration of competing interest

No conflicts of interest to disclose.

Acknowledgements

The material presented in this paper is a result of the PhD research by

References

Allcock, J.B., 1982. Skarn and porphyry Cu mineralization at Mines Gaspé, Murdochville, Quebéc. Econ. Geol. 77, 971–999.

Armbruster, Thomas, et al., 2006. Recommended nomenclature of epidote-group minerals. Eur. J. Mineral. 18, 551–567. https://doi.org/10.1127/0935-1221/2006/0018-0551.

Bendezú, R., Fontboté, L., 2002. Late timing for high sulfidation Cordilleran base metal lode and replacement deposits in porphyry-related districts: the case of Colquijirca, central Peru. In: Society for Geology Applied to Mineral Deposits News, 13, pp. 9–13.

Bourque, P.-A., Brisebois, D., Malo, M., 1995. Gaspé Belt. In: Williams, H. (Ed.), Geology of the Appalachian–Caledonian Orogen in Canada and Greenland, Geological Survey of Canada, Geology of Canada, No. 6, pp. 316–351, 5 p.

Carroll, J.I., 2003. Geology of the Kedgwick, Gounamitz River, States Brook and Menneval map areas (NTS 21 O/11, 21 O/12, 21 O/13 and 21 O/14), Restigouche County, New Brunswick. In: Carroll, B.M.W. (Ed.), Current Research, 2002. New Brunswick Department of Natural Resources; Minerals, Policy and Planning Division, pp. 23–57. Mineral Resource Report 2003-4.

Desrosier, C., 2013. In: Results of the 2013 Exploration Program on the Legacy and Burntland Properties. Christian Desrosier Géologue-Conseil Inc., New Brunswick, Canada, p. 80.

Einaudi, M.T., 1982. Description of skarns associated with porphyry copper plutons, southwestern North America. In: Titley, S.R. (Ed.), Advances in Geology of the

Porphyry Copper Deposits, Southwestern North America. University of Arizona Press, Tucson, AZ, pp. 139–184.

Einaudi, M.T., Meinert, L.D., Newberry, R.J., 1981. Skarns Deposits: Economic Geology, 75th Anniversary Volume, 317–391p.

Fyffe, L.R., Fricker, A., 1987. Tectonostratigraphic terrane analysis of New Brunswick. Marit. Sediments Atl. Geol. 23, 113–122.

Girard, P., 1971. The Madeleine Cu mine, Gaspé, Québec: A hydrothermal deposit. Unpublished PhD thesis. McGill University, Montréal, Canada, 243 p.

Gower, S.J., Walker, J.A., 1993. Skarn-type base-metal deposits in northern N.B. Geology and skarn occurrences. In: McCutcheon, S.R., Woods, G.A. (Eds.), Guidebook to the porphyry copper and copper skarn mineralization in northern New Brunswick and Gaspé, Québec: Geological Society of the Canadian Institute of Mining, Metallurgy and Petroleum, 3rd Annual Field Conference, Trip #1 of Bathurst '93, 5–21pp.

Hibbard, J.P., van Staal, C.R., Rankin, D.W., Williams, H., 2006. Lithotectonic map of the Appalachian Orogen, Canada–United States of America. Geological Survey of Canada. Map 2096A, scale 1:1 500 000.

Hollister, V.F., 1978. In: Geology of the Porphyry Cu Deposits of the Western Hemisphere. American Institute of Mining, Metallurgical and Petroleum Engineers, New York, p. 219.

Hollister, V.F., Potter, R.R., Barker, A.L., 1974. Porphyry-type deposits of the Appalachian orogeny. Econ. Geol. 69, 618–630.

Kwak, T.A.P., 1986. Fluid inclusions in skarns (carbonate replacement deposits). J. Metamorph. Geol. 4, 363–384.

Leake, B.E., Woolley, A.R., Birch, W.D., Burke, E.A.J., Ferraris, G., Grice, J.D., Hawthorne, F.C., Kisch, H.J., Krivovichev, V.G., Schumacher, J.C., Stephenson, N.C.N., Whittaker, E.J.W., 2004. Nomenclature of amphiboles: additions and revisions to the International Mineralogical Association's amphibole nomenclature. Eur. J. Mineral. 16, 191–196.

Lentz, D., Walker, J.A., Stirling, J.A.R., 1995. Millstream Cu-Fe skarn deposit: an example of a Cu-bearing magnetite-rich skarn system in northern New Brunswick. Explor. Min. Geol. 4, 15–31.

Malo, M., Moritz, R., Roy, F., Chagnon, A., 1993. Géologie et mètallogènie du segment est de la faille du Grand Pabos. Ministère de l'Énergie et des Ressources du Québec Report MB 93-55, Gaspésie, 123 p.

Malo, M., Moritz, R., Dubé, B., Chagnon, A., Roy, F., Pelchat, C., 2000. Base metal skarns and au occurrences in the Southern Gaspé Appalachians: distal products of a faulted and displaced magmatic-hydrothermal system along the Grand Pabos-Restigouche Fault System. Econ. Geol. 95, 1297–1318.

Massawe, R.J., Lentz, D.R., 2019. Petrochemistry and U-Pb (zircon) age of porphyry dykes at the McKenzie Gulch porphyry – skarn Cu-Ag-Au deposit, north-central New Brunswick, Canada: implications for emplacement age, tectonic setting and mineralization potential. Can. J. Earth Sci. 57, 427–452.

Massawe, R.J., Lentz, D.R., 2020. Evaluation of crystallization and emplacement conditions of the McKenzie Gulch porphyry dykes using chemistry of rock-forming minerals: implications for mineralization potential. Ore Geol. Rev. 116, 1–18.

Massawe, R.J., Lentz, D.R., 2021. Petrogenesis and U–Pb (titanite) age of Cu–Ag skarn mineralization in the McKenzie Gulch area, northern New Brunswick, Canada. Under Review.

Mcllreath, I.A., James, N.P., 1984. Carbonate slopes. In: Walker, R.G. (Ed.), Facies Models, Geoscience Canada, Reprint Series, Second edition, 1, pp. 245–257.

Meinert, L.D., 1983. Variability of skarn deposits: guides to exploration. In: Boardam, S.J. (Ed.), Revolution in the Earth Sciences. Kendall-Hunt, Dubuque, Iowa, pp. 301–316.

Meinert, L.D., Hedenquist, J.W., Satoh, H., Matsuhisa, Y., 2003. Formation of anhydrous and hydrous skarn in Cu-Au ore deposits by magmatic fluids. Econ. Geol. 98, 147–156.

Moore, C.E., Lentz, D.R., 1996. In: Cu-skarn-associated felsic intrusive rocks in the McKenzie Gulch area (NTS 21 O/10), Restigouche County, New Brunswick. New Brunswick Department of Natural Resources and Energy, Minerals and Energy Division, pp. 121–153.

Procyshyn, E.L., 1987. Wall rock alteration mineral assemblages associated with the E-zone ore bodies at Mines Gaspé, Murdochville, Quebec. Geological Survey of Canada. Paper 87-1A, 499–514p.

Ray, G.E., Webster, I.C.L., 1997. Skarns in British Columbia. British Columbia Geological Survey Branch Bulletin, 101, 260 p.

Roy, F., 1991. Synthèse structurale et métallogénique de l'indice Reboul. Unpublished Mémoire de M.Sc. Université Laval, Québec, 91p.

Rusk, B., Reed, M., 2002. Scanning electron microscope-cathodoluminescence analysis of quartz reveals complex growth histories in veins from the Butte porphyry copper deposit, Montana. Geology 30, 727–730.

Savard, M., 1985. Indices minéralisés du sud de la Gaspésie. Ministère de l'Énergie et des Ressources du Québec Report ET 83-08, 92 p.

Shelton, K.L., 1983. Composition and origin of ore-forming fluids in a carbonate-hosted porphyry Cu and skarn deposit: a fluid inclusion and stable isotope study of Mines Gaspé, Québec. Econ. Geol. 78, 387–421.

Shelton, K.L., Rye, D.M., 1982. Sulfur isotope compositions of ores from Mines Gaspé, Québec: an example of sulfate-sulfide isotopic disequilibria in ore-forming fluids with applications to other porphyry-type deposits. Econ. Geol. 77, 1688–1709.

Stow, D.A.V., Lovell, J.P.B., 1979. Contourites: their recognition in modern and ancient sediments. Earth-Sci. Rev. 14, 251–291.

Wares, R., Brisebois, D., 1998. Geology and metallogeny of the Cu-porphyry-related Mines Gaspé, Murdochville, Gaspésie. In: Geological Association of Canada-Mineralogical Association of Canada Joint Annual Meeting, Québec. Field Trip B4 Guidebook.

Williams-Jones, A.E., 1982. Patapédia: an Appalachian calc-silicate-hosted Cu prospect of porphyry affinity. Can. J. Earth Sci. 19, 438–455.

Wilson, R.A., 2002. Geology of the Squaw Cap area (NTS 21 O/15d, e, f), Restigouche County, New Brunswick. In: Carroll, B.M.W. (Ed.), Current Research 2001. New Brunswick Department of Natural Resources and Energy; Minerals, Policy and Planning Division, pp. 155–196. Mineral Resource Report, 2002-4.

Wilson, R.A., 2017. The Middle Paleozoic Rocks of Northern and Western New Brunswick, Canada. New Brunswick Department of Energy and Resource Development; Geological Surveys Branch. Memoir 4, 319 p.

Wilson, R.A., Kamo, S.L., 2008. New U–Pb ages from the Chaleurs and Dalhousie groups: implications for regional correlations and tectonic evolution of northern New Brunswick. In: Martin, G.L. (Ed.), Geological Investigations in New Brunswick for 2007. New Brunswick Department of Natural Resources; Minerals, Policy and Planning Division. Mineral Resource Report, 55–77p.

Wilson, R.A., Burden, E.T., Bertrand, R., Asselin, E., McCracken, A.D., 2004. Stratigraphy and tectono-sedimentary evolution of the Late Ordovician to Middle Devonian Gaspé Belt in northern New Brunswick: evidence from the Restigouche area. Can. J. Earth Sci. 41 (5), 527–551.

Woods, G.A., 1993. Skarn-type base-metal deposits in northern New Brunswick. Skarn type base metal deposits in the McKenzie Gulch, Patapédia and Popelogan areas. In: McCutcheon, S.R., Woods, G.A. (Eds.), Guidebook to the porphyry copper and copper skarn mineralization in northern New Brunswick and Gaspé, Québec, Geological Society of the Canadian Institute of Mining, Metallurgy and Petroleum, 3rd Annual Field Conference, Trip #1 of Bathurst, '93, pp. 42–53.